Journal of the European Ceramic Society **19** (1999) 2265–2272

PII: S0955-2219(99)00119-3
0955-2219/99/$ - see front matter

Structural Correlations at Si/Si_3N_4 Interface and Atomic Stresses in Si/Si_3N_4 Nanopixel-10 Million-atom Molecular Dynamics Simulation on Parallel Computers

Martina E. Bachlechner,[a,*] Rajiv K. Kalia,[a] Aiichiro Nakano,[a] Andrey Omeltchenko,[a] Priya Vashishta,[a] Ingvar Ebbsjö,[b] Anupam Madhukar[c] and Guang-Lin Zhao[d]

[a]Concurrent Computing Laboratory for Materials Simulations, Department of Physics and Astronomy, and Department of Computer Science, Louisiana State University, Baton Rouge, LA 70803-4001, USA
[b]Studsvik Neutron Research Laboratory, University of Uppsala, S-611 82 Nyköping, Sweden
[c]Department of Materials Science and Engineering, University of Southern California, Los Angeles, CA 90089-0241, USA
[d]Department of Physics, Southern University and A & M College, Baton Rouge, LA 70813, USA

Abstract

We have combined first-principle calculations of charge transfer at the Si/Si_3N_4 interface with the interaction potential models for bulk Si and Si_3N_4 to produce a model for the Si/Si_3N_4 interface. Using these interatomic potentials, million atom molecular dynamics simulations have been performed to characterize the structure of $Si(111)/Si_3N_4(0001)$ and the $Si(111)/a\text{-}Si_3N_4$ interfaces. Ten million-atom simulations are performed using multiresolution molecular-dynamics method on parallel computers. Atomic stress distributions are determined in a 54 nm nanopixel on a 0·1 μm silicon substrate. Effects of surfaces, edges, and lattice mismatch at the $Si(111)/Si_3N_4(0001)$ interface on the stress distributions are also investigated. Stresses are found to be highly inhomogeneous in the nanopixel—the top surface of silicon nitride has a compressive stress of $+3\,GPa$ and the stress is tensile, $-1\,GPa$, in silicon below the inter-face. These simulation methods can also be applied to other semiconductor/ceramic interfaces as well as to metal/ceramic and ceramic/ceramic interfaces. © *1999 Elsevier Science Ltd. All rights reserved.*

Keywords: molecular dynamics, Si, Si_3N_4/Si interface, simulation, Si_3N_4.

*To whom correspondence should be addressed.

1 Introduction

In silicon electronics, spatial inhomogeneities in the dopant distribution are of great importance for the device characteristics when the pixel sizes become smaller than 100 nm.[1] Rapidly varying stresses at and near edges originating from this nanoscale pixellation may lead to defect formation or even initiate a crack.[2] Understanding the stress distribution is therefore essential in the design of nanoscale devices.

Utilizing the framework of linear elasticity and finite-element (FE) simulations,[3,4] edge stresses in Si/SiO_2 and Si/Si_3N_4 have been examined on length scales larger than 1 μm. For nanoscale devices, however, the surface-to-volume ratio is so large that the influence of surfaces, edges and corners on elastic properties becomes significant. Due to chemical bonding at the Si/Si_3N_4 interface, types of stresses not present in silicon or silicon nitride materials are introduced. These effects have to be included in constitutive relations to achieve realistic description of nanoscale devices in the FE approach.

An alternative approach is to use molecular-dynamics simulations, where surface and interface bonding effects are explicitly included at the atomistic level. With recent progress in parallel computer architectures, it has now become possible to carry out direct atomistic simulations for submicron structures with realistic descriptions of the materials involved. In particular, large-scale MD simulations have proven to be useful in the study of dynamic

fracture.[5] MD simulations provide spatially resolved stress distributions on the length scales not accessible to experimental techniques, such as MicroRaman spectroscopy.[6,7] Such numerical experiments can be used to establish the validity of constitutive relations used in FE simulations, in particular the treatment of surface/interface/edge effects.

Within MD simulations, the crucial ingredient is the determination of a reliable interatomic potential. In the case of Si_3N_4 the potential consists of two parts: The two-body interaction consisting of a screened Coulomb term, charge-dipole interaction and steric repulsion and the three body part of the interaction consisting of bond-bending and bond-stretching terms. The potential used in the present investigation[8] provides a good description of the structural and mechanical properties and dynamical behavior,[9,10] (static structure factor, bulk and Young's moduli, and phonon density of states) and fracture behavior of crystalline and amorphous Si_3N_4.[11–14] For silicon we have used the well-known Stillinger-Weber interaction potential.[15]

Across the silicon/silicon nitride interface a reasonable interaction had to be developed. Originally, a Si atom in bulk silicon does not have any ionic character, the bonding attribute in bulk silicon being covalent. However, the Si atoms at the interface become partially ionic when forming bonds with the N atoms of silicon nitride across the interface. To have an estimate of the fractional ionic character electronic structure calculations have been performed on the Si/Si_3N_4 interface which will be discussed in Section 2. In Section 3 we present MD simulation results for structural correlations at the interface and for spatial stress distributions in nanopixels. A conclusion is presented in Section 4.

2 Electronic Structure and Charge Transfer in Si/Si_3N_4

2.1 LCAO electronic structure calculations and charge transfer in bulk Si_3N_4

The LCAO (linear combination of atomic orbitals) method is based on using atomic orbitals as the basis to expand the electronic eigenfunction of a many-atom system. The exchange-correlation interaction of the many-electron system is described by the density functional theory in a local density approximation. Therein, the Ceperley–Alder form of the exchange-correlation potential is used. The LCAO method is very attractive in dealing with complex insulator and semiconductor materials with a large number of atoms per unit cell. The details of the LCAO calculations reported here are described in Ref.16.

The α-phase silicon nitride has a hexagonal structure with 28 atoms per unit cell.[17] The lattice constants are $a = 7{\cdot}818$Å and $c = 5{\cdot}591$Å. In the self-consistent calculation, a mesh of 20 k-points with the proper weights in the irreducible Brillouin zone was used. A comparison of the total energy with a test using a mesh of 5 k-points only revealed a small difference of about 0·00001 Ry. This is an indication of satisfactory convergence with respect to the number of k-points.

From the calculated electronic band structure of α-phase Si_3N_4, the direct band gap at the Γ point can be determined to be about 4·7 eV. It is very close to the smallest indirect band gap of other transitions and lies in the range of experimental values.[18]

Using the LCAO eigenfunctions, the effective charge of an atom is obtained and the charge transfer is determined as the difference of the effective charge and the neutral charge of the atom. We find that the silicon atoms give about 1·23 to 1·25 electrons/atom; nitrogen atoms gain about 0·91 to 0·94 electrons/atom. Based on the charge transfer, the ionic formula for the silicon nitride may be then written as $Si_3^{+1{\cdot}24}\ N_4^{-0{\cdot}93}$. The estimated error in the calculation of the charge transfer is $\cong 10\%$.

For one Si–N bond, the silicon atom transfers about 0·31 electrons to the nitrogen atom. This calculated value of charge transfer for one Si–N bond is very close to the so called 'one-third rule' in silicon nitride, which is extracted from experimental data and used in molecular dynamics simulations.

2.2 Free Si_3N_4(0001) surface

Before turning to the complex structure of the $Si(111)/Si_3N_4$ interface, the Si_3N_4(0001) surface is examined. Both the α- and β-phase Si_3N_4 have a layered structure in the hexagonal lattice.[17] One sheet of Si_3N_4 has three silicon atoms bonded to four nitrogen atoms. The inter-layer interaction is weaker than the intra-layer interaction. It is energetically more favorable to cleave or grow silicon nitride in a layer structure. The surface of Si_3N_4 will be one sheet of silicon nitride. On the top of the surface, three nitrogen atoms and three silicon atoms have dangling bonds. The fourth nitrogen atom is bonded to three silicon atoms on the layer and has no dangling bond.

For the electronic structure of the unrelaxed Si_3N_4(0001) surface, twenty-eight atoms in one unit cell of the two dimensional Si_3N_4(0001) slate were used to simulate the free surface structure.

The self-consistent calculation[16] revealed that the charge transfer from the surface silicon atoms (having one dangling bond) is about 1·10 electrons/

Si-atom which is smaller than the silicon charge transfer (1·24) in the bulk Si_3N_4. Correspondingly, the surface nitrogen atoms with one dangling bond gain about 0·79 electrons/N-atom which is also smaller than the charge transfer of the N atom (0·93) in the bulk. It is interesting to see that the fourth surface nitrogen atom without a dangling bond gains about 0·94 electrons/N-atom which is very close to the charge gain of a nitrogen atom in bulk Si_3N_4. We conclude that the reduced charge transfer for the other surface nitrogen atoms and for the silicon atoms can be attributed to their dangling bonds.

2.3 Si(111)/Si_3N_4(0001) interface

In this study using the LCAO method, a supercell of 52 atoms for the interface structure was used. Six layers of Si 2×2 (111) containing 24 atoms were matched to four layers of Si_3N_4(0001). The lattice mismatch of the two materials is only about 1%. Since the silicon nitride is stiffer than the silicon crystal, the Si(111) layers were expanded along x and y directions to match the Si_3N_4 lattice parallel to the interface. In the x–y plane parallel to the interface, periodic boundary conditions were applied. Outside of the Si(111) and Si_3N_4(0001) layers there is an empty space in the supercell.

A Si 2×2(111) layer has four Si atoms/cell. Three of the four Si atoms (small light red spheres in Fig. 1) of the first Si(111) layer near the interface directly bond to the three N atoms (large light yellow spheres) of Si_3N_4(0001) layer as shown in Fig. 1. Each of these nitrogen atoms has one dangling bond before matching the Si(111) layer onto the Si_3N_4(0001) surface. The fourth Si atom of the first Si(111) layer is on top of another N atom which is bonded to three Si atoms of the first Si_3N_4 sheet. The three Si atoms (the small light blue spheres) of the interfacial Si_3N_4 plane still have one dangling bond that generates the defects of $\bullet\,\mathrm{Si} \equiv \mathrm{N}_3$.[19]

Within the self-consistent LCAO method for the Si(111)/Si_3N_4(0001) interface, three k-points with proper weights in the two-dimensional Brillouin zone were used. A comparison with results of the one k-point (Γ point) calculation showed only a small difference of the charge distribution. The calculated DOS spectrum of Si 2p core levels for the Si(111)/Si_3N_4(0001) interface is in good agreement with XPS experiments. The Si 2p levels in the Si_3N_4 side shift down about 3·1 to 3·5 eV relative to the Si 2p states of Si(111) side.

Some contour plots of the valence charge density for the Si(111)/Si_3N_4(0001) interface structure are shown in Figs. 2–4. A two-dimensional contour diagram of the valence charge density on a plane perpendicular to the interface is given in Fig. 2. This plane cuts through two nitrogen atoms of the interfacial Si_3N_4 plane and two silicon atoms on the interfacial Si(111) plane. This clearly indicates that the charge density near the nuclei changes rapidly. It is evident from Figs. 2 and 3 that the size of a nitrogen atom is much larger than that of a silicon atom. The sizes of the silicon and nitrogen atoms may be estimated as $R_N = 1{\cdot}15$ Å and $R_{si} = 0{\cdot}61$Å, respectively. The bonding behavior of the Si and N atoms near the interface can be seen from the relatively denser distribution and a more complex structure of the contour lines than that of the interstitial region. The electron charge in the bonding area can not be clearly associated with a

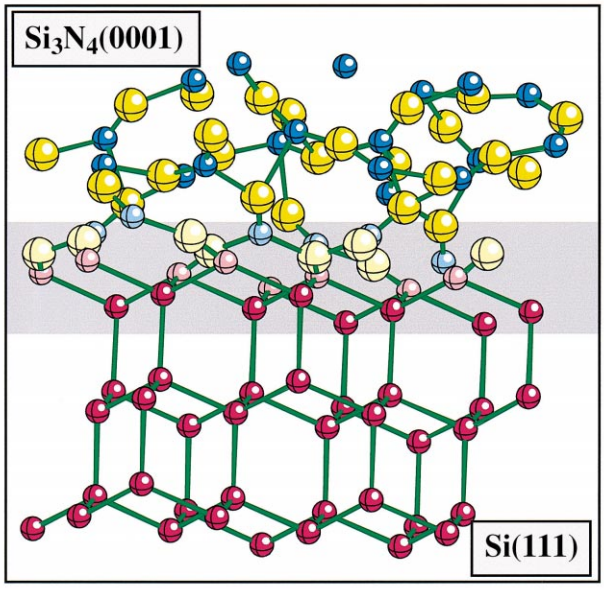

Fig. 1. The atomic structure of the Si(111)/Si_3N_4(0001) interface used in the study. The small red spheres are the Si(111) atoms; the small blue shaded spheres are the Si atoms of the Si_3N_4 side; and the large yellow spheres are the N atoms of the Si_3N_4 side. The interface region is indicated by a grey strip.

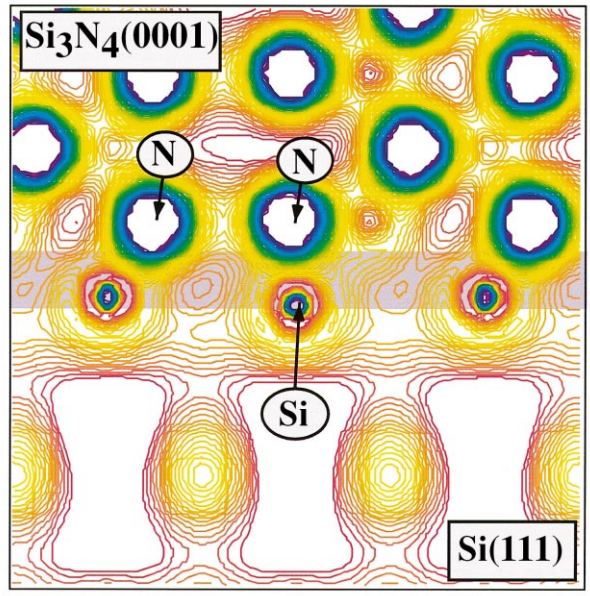

Fig. 2. The valence charge density map on a two dimensional plane perpendicular to the Si(111)/Si_3N_4(0001) interface.

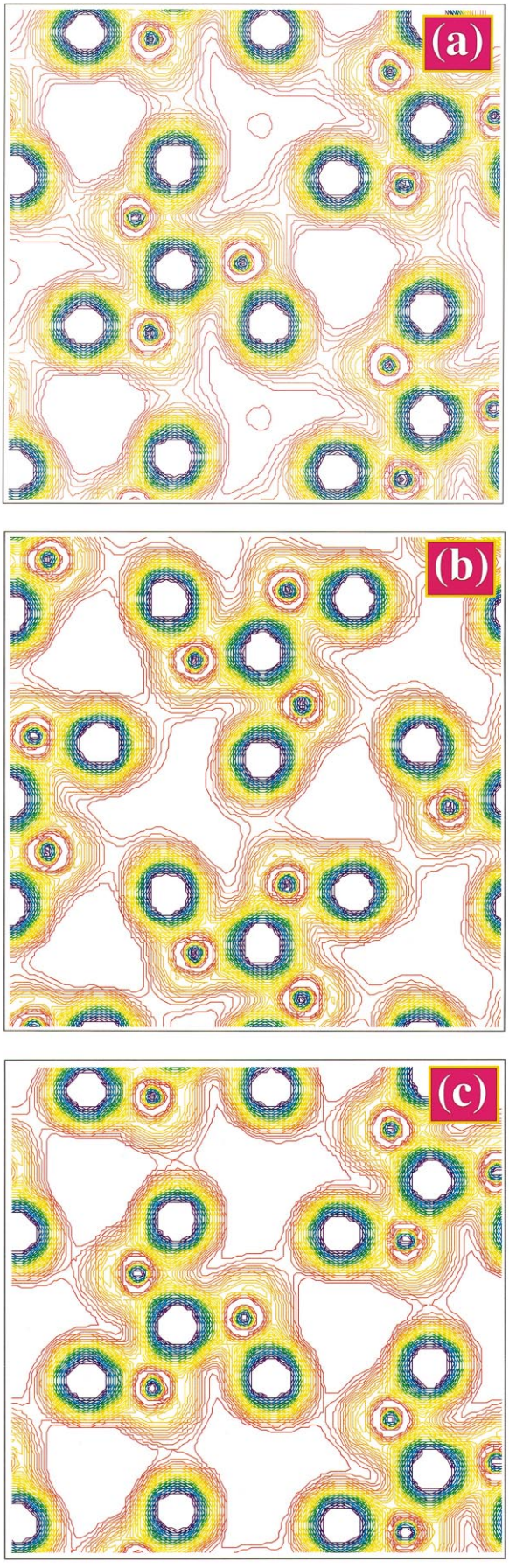

Fig. 3. The valence charge density maps on the Si_3N_4 side near the interface. These planes are parallel to the $Si(111)/Si_3N_4(0001)$ interface. (a) The first Si_3N_4 sheet; (b) the second Si_3N_4 sheet away from the interface, (c) the third Si_3N_4 sheet away from the interface.

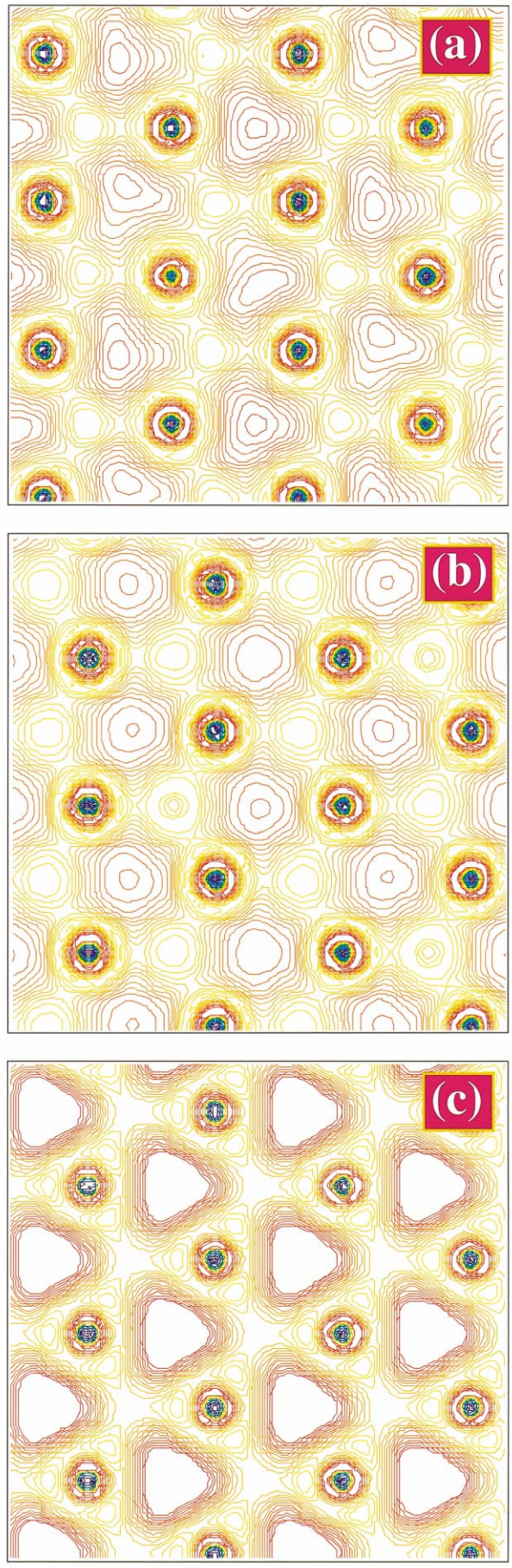

Fig. 4. The valence charge density on the Si(111) side. All the planes are parallel to the interface. (a) The first Si(111) layer near the interface; (b) the second Si(111) layer away from the interface structure (c) the third Si(111) layer away from the interface structure.

specific atom. This is a manifestation of partially covalent nature of the bond.

Figure 3 shows valence charge density maps of three planes of Si_3N_4 parallel to the interface, with Fig. 3(a) being for the interfacial plane. The formation of the Si–N bond can be seen from the distribution of the contour lines. One N atom is fully bonded to three Si atoms on the Si_3N_4 plane. The other three N atoms on the interfacial Si_3N_4 plane [Fig. 3(a)] have one bond to a Si atom on the same plane, and one bond to the Si atom of the Si_3N_4 plane above. It also has one bond to the Si atom of the Si(111) layer which is below the first Si_3N_4 plane. For the second and third planes [Fig. 3(b) and (c)] these N atoms have bonds to the Si_3N_4 planes lying above and below.

The valence charge density on the silicon side parallel to the interface is shown in Fig. 4, with Fig. 4(a) being the interfacial plane. The hexagonal structure of the Si(111) layer is reflected in Fig. 4. The Si atoms do not bond to each other on this plane as seen from the distribution of the charge density. All the bonds are pointing out of the plane. Whereas the first layer indicates the influence of the interface on the charge density [Fig. 4(a)], the third layer clearly represents the electronic structure of a bulk like behavior, namely high charge density around the atom positions and low one in the interstitial regions [cf. Fig. 4(c)].

Three of the Si atoms from the interfacial Si(111) plane lose about 0·41 to 0·44 electrons. These three Si atoms are bonded to three N atoms of the interfacial Si_3N_4 plane by giving away some electrons. Otherwise these three N atoms would have a dangling bond at the Si_3N_4 surface. The remaining Si atom at the interfacial plane in silicon has only a charge transfer of about 0·26 electrons which is much smaller than the other three Si atoms. This Si atom is on top of the N atom which is fully bonded to three Si atoms of Si_3N_4 side and has no dangling bond before the matching of the Si(111) plane to the Si_3N_4 surface.

The charge transfer for the four Si atoms on the second Si(111) plane from the interface is small. The Si atoms at the third and fourth Si(111) layers away from the interface have no noticeable charge transfer within the calculation uncertainty. This is an indication that the Si atoms in these two layers at the middle of Si(111) film are very close to the bulk properties.

It was found that the N atoms at the interface have a charge transfer very close to the value of the N atom charge gain in the bulk silicon nitride. Three of these N atoms gain about 0·93 electrons/atom, the fourth N atom has a smaller charge transfer of 0·84 electrons/atom; this inhomogeneity is largely due to the mismatch of the interface. It was found that one Si–N bond would be assigned a charge transfer of about 0·31 electrons which is that of bulk Si_3N_4. The three Si atoms at the interfacial Si_3N_4 plane have a charge transfer of about 0·73 to 0·89 electrons, which is much smaller than the Si charge transfer in the bulk Si_3N_4. Even the charge transfer of these Si atoms of silicon nitride at the interface is smaller than the case of the Si atoms at the free Si_3N_4 surface. Further analysis of the data showed that these three Si atoms of the silicon nitride side gained some electrons from the Si(111) atoms. The effective charge of the Si and N atoms at the second and third Si_3N_4 planes away from the interface [Figs. 3(b) and 3(c)] is very close to the case of bulk Si_3N_4.

3 Molecular Dynamics Simulations of the Si/Si_3N_4 Interface and Si/Si_3N_4 Nanopixel

3.1 Structural correlations at the Si/Si_3N_4 interface

Bulk Si_3N_4 is modeled using a combination of two- and three-body interactions which include charge transfer, electronic polarizability and covalent bonding effects.[8] To describe the bonding across the Si/Si_3N_4 interface, the interface atoms are treated differently from those in the bulk. For the silicon system we describe the interactions by the Stillinger–Weber potential.[15]

The initial configuration for our molecular dynamics simulation are crystalline Si(111) and $Si_3N_4(0001)$ that are placed at a distance of 6 Å from each other. The silicon system of size 162 Å × 233 Å × 38 Å consists of 69 120 particles, the Si_3N_4 system of the same size contains 141 120 particles. The two systems are separately relaxed to a zero-force configuration using the steepest-descent approach. Then the separation distance is reduced to 1·5 Å in steps of 0·5 Å. At each step, the system is quenched to zero temperature. A short time step of 1 fs had to be used in order to prevent that particles from the free surfaces fly away and particles at the interface enter the other system before interacting with the interface particles. Subsequently, the system is heated and thermalized at 300 K using the Langevin dynamics.

The $Si(111)/Si_3N_4(0001)$ interface structure is characterized by calculating bond-length and bond-angle distributions. Figure 5(a) shows a schematic view of the interface. Silicon atoms on the Si(111) surface form bonds with N atoms in Si_3N_4. There are two different types of such bonds [indicated by the dashed and cross-hatched underlying ellipses in Fig. 5(a)]. The bond-length distributions for the two types of bonds across the interface are shown in Figs. 5(b) and 5(c). The Si–N bond length across the interface is close to that in bulk Si_3N_4(1·73 Å).

3.2 Stress distribution in a Si/Si_3N_4 nanopixel

The main issue we address in these simulations is the local stress distribution in a Si(111)/Si_3N_4(0001) nanopixels.[20] An efficient algorithm for parallel architectures has been developed to handle multimillion-atom molecular dynamics simulations for the Si/Si_3N_4 system. Additional computational speedup is achieved by using a multiple-time step approach[21] to exploit the separation of time scales and Langevin dynamics approach to reduce the length of equilibration runs for inhomogeneous systems.

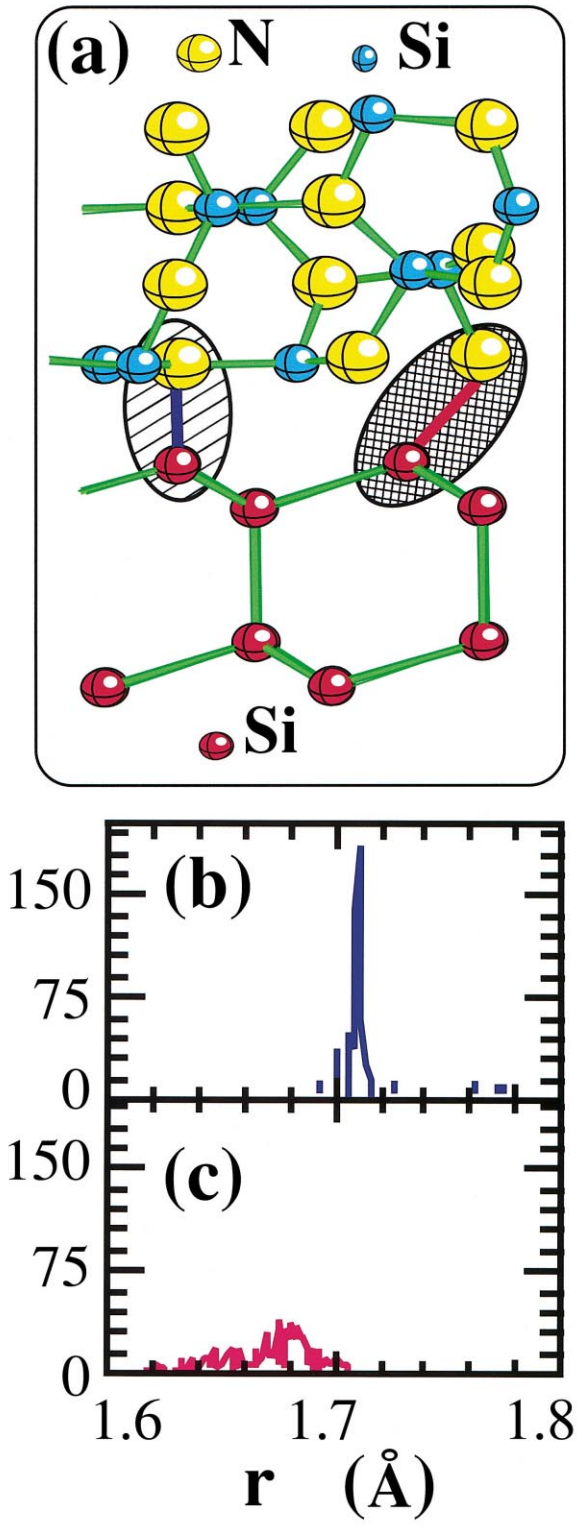

Fig. 5. (a) Si(111)/Si_3N_4(00001) interface. (b) and (c) Si–N bond length distribution for two different bonds marked by striped and dotted ellipses in (a).

The simulated system consists of a 540 Å×327 Å×133 Å Si mesa on top of a 1077 Å×653 Å×230 Å Si(111) substrate (see Fig. 6). Periodic boundary conditions are used in the plane of the substrate. The top surface of the mesa is covered with a 83 Å-thick α-crystalline Si_3N_4(0001) film. The lattice Si(111)/Si_3N_4(0001) interface involves a 1·1% lattice mismatch (2×2 unit cell of Si is slightly smaller than one unit cell of Si_3N_4). We have also considered a reference system where the parameters of the Si potential are modified so that the lattice constants of Si and Si_3N_4 match exactly. This procedure allows us to isolate the effect of the lattice mismatch on the interfacial stress distribution.

The nanopixel is prepared in the same way as the interface described above. Atomistic-level stresses are then calculated for the two cases of mesas without and with lattice mismatch. The stresses in Si and Si_3N_4 are averaged over the appropriate unit cells, which is necessary to obtain meaningful stress distributions in the case of binary systems such as Si_3N_4 which have atoms of widely different sizes.

Figure 7(a) shows the spatially resolved stress in the absence of the lattice mismatch. Here the stresses are primarily due to the surface effects. In addition, the stress distribution contains stress singularities near the edges of the mesa/substrate boundary. The 1·1% Si/Si_3N_4 lattice mismatch introduces additional contributions to the stress at the interface: compressive stress in Si_3N_4 and tensile stress in Si [Fig. 7(b)]. The mismatch-induced stress penetrates deep into the Si mesa to form a tensile stress well.

The hydrostatic $[(\sigma_{xx}+\sigma_{yy}+\sigma_{zz})/3]$ and in-plane $[(\sigma_{xx}+\sigma_{yy})/2]$ stresses along the z-axis through the center of the nanopixel are plotted in Fig. 8. The

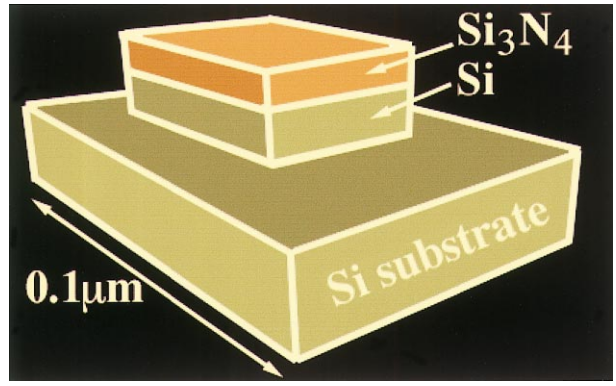

Fig. 6. Schematics of the Si/SiS/Si_3N_4 nanopixel.

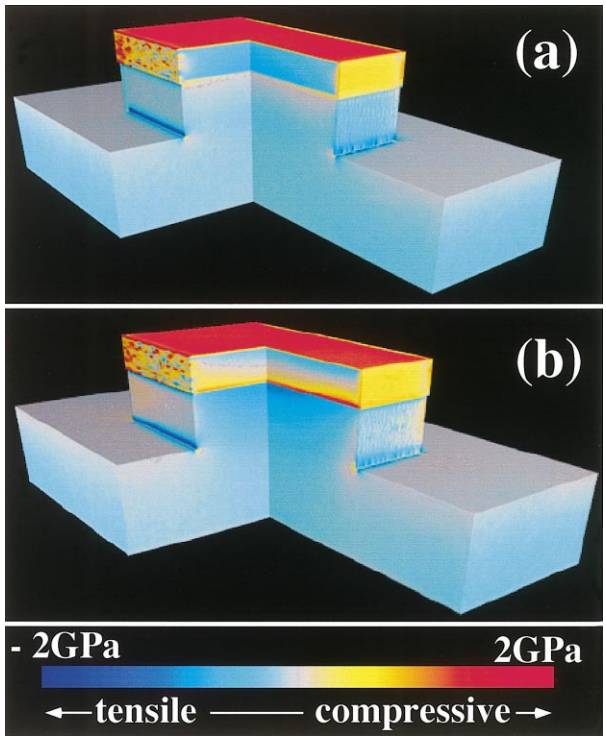

Fig. 7. Stress distribution in a Si/Si/Si_3N_4 nanopixel, (a) without lattice mismatch and (b) in the presence of the 1·1% lattice mismatch. To show the stresses inside the nanopixel one quarter of the system is removed.

stress in the absence of the lattice mismatch is shown in Fig. 8(a). The top surface of the Si_3N_4 film is subject to a strong compressive stress due to repulsive forces between the N atoms on the surface. Additional stress contributions arise due to intrinsic stress at the interface. As a result, the interior of the Si_3N_4 film experiences tensile stress. The lattice mismatch results in an additional compressive stress in Si_3N_4 above the interface and tensile stress in Si [Fig 8(b)]. To isolate the effect of the lattice mismatch, we subtract the stress in the lattice matched system [Fig. 8(a)] from the lattice mismatched data of Fig 8(b). The resulting stress contribution shown in Fig. 8(c) is entirely due to the lattice mismatch. The magnitude and spatial variation of this mismatch-induced stress is consistent with linear elasticity estimates and finite element calculations.[3,4]

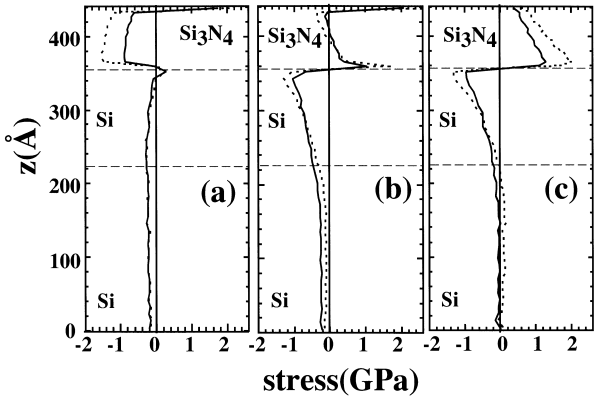

Fig. 8. Hydrostatic $[(\sigma_{xx}+\sigma_{yy}+\sigma_{zz})/3$ (solid curve) and in-plane $[(\sigma_{xx}+\sigma_{yy})/2]$ (dashed curve) stresses along the z-axis through the center of the nanopixel. (a) lattice matched Si(111)/Si_3N_4(001) interface, (b) lattice mismatched Si(111)/Si_3N_4(0001) interface, and (c) difference of lattice matched and mismatched interfaces.

4 Conclusions

The electronic structure, the charge distribution, and the charge transfer in Si_3N_4, at the free Si_3N_4 surface, and for the interface structure of Si(111)/Si_3N_4(0001) have been studied using the self-consistent LCAO method. It is found that the silicon atoms in Si_3N_4 lose about 1·24 electrons/N-atom to the nitrogen atoms which gain about 0·93 electrons/N-atom. The ionic formula for the silicon nitride may be written as $Si_3^{+1.24}N_4^{-0.93}$. At the Si(111)/Si_3N_4(0001) interface, the Si atoms on the silicon side lose some electrons to the N atoms of the silicon nitride side and form Si–N bonds across the interface. The calculated results show that one Si–N bond would associate with a charge transfer of about 0·31 electrons/bond from the Si atom to the N atom, which is the same as the bulk Si_3N_4 value.

Using these charge transfer values, an interface model has been developed to describe the interaction between the two interfacing systems. To characterize the interface, we have calculated bond-length and bond-angle distributions showing the formation of bonds across the interface.

Ten million-atom molecular dynamics simulations using the space-time multiresolution algorithms have been performed on parallel computers to investigate the stress distribution in a Si(111)/Si_3N_4(0001) mesa on Si(111) substrate. Stress concentration is observed near the interface and at the mesa/substrate edges. A lattice mismatch of 1·1% at the Si(111)/Si_3N_4(0001) interface manifests as a stress well in the center of the mesa. Additional simulations are currently under way to study different geometries of the nanopixel and the effect of amorphous Si_3N_4 in place of crystalline silicon nitride.

Acknowledgements

Work supported by the Austrian FWF (J01146-PHY and J01444-PHY), DOE (Grant No. DE-FG02-96ER-45570), NSF (Grant No. DMR-9711903), AFOSR (Grant No. F 962098-1-0086), USC-LSU MURI (Grant No. F 49620-95-1-0452), ARO (Grant No. DAAH04-96-1-0393), PRF

(Grant No. 31659-AC9), and NASA (NAG2-1212, NAG21248). The 10 million-atom simulations were carried out at the 256-processor HP Exemplar at Caltech. Access to the Exemplar was provided by the National Partnership for Advanced Computational Infrastructure (NPACI) through a cooperative agreement from the National Science Foundation.

References

1. Ferry, D. K. and Goodnick, S. M. *Transport in Nanostructures* (Cambridge University Press, 1997).
2. Liu, F, Wu, F. and Lagally, M. G., Effect of strain on structure and morphology of ultrathin Ge films on Si(001). *Chem. Rev*., 1997, **97**, 1045–1061.
3. DeWolf, I., Vanhellemont, J. and Romano-Rodriguez, A., *J. Appl. Phys*., 1997, **71**, 898.
4. Jain, S. C., Harker, A. H., Atkinson, A. and Pinardi, K., Edge-induced stress and strain in stripe films and substrates: A two-dimensional finite element calculation. *J. Appl. Phys*., 1995, **78**, 1630–1637.
5. Selinger, R. L. B., Mecholsky, J. J., Carlsson, A. E. and Fuller, E. R., *Fracture - instability, scaling, and ductile/brittle behavior* (MRS, Pittsburgh, 1996).
6. Tang, W. C., Rosen, H. C. and Guha, S., Raman microprobe study of narrow: In_xGa_{1-x} stripes on patterned GaAs(100) substrates. *Thin Solid Films*, 1991, **231**, 8.
7. Rupp, T., Kaesen, F., Hansch, W., Gravesteijn, D. J., Schorer, E., Silveira, G., Abstreiter, G. and Eisele, I., Defect-free strain relaxation in locally MBE-grown SiGe heterostructures. *Thin Solid Films*, 1997, **294**, 27.
8. Vashishta, P., Kalia, R. K., Nakano, A., Li, W. and Ebbsjö, I. In *Amorphous Insulators and Semiconductors*, ed. M. F. Thorpe and M. I. Mitkova (NATO ASI, 1996).
9. Vashishta, P., Kalia, R. K. and Ebbsjö, I., Low-energy floppy modes in high-temperature ceramics. *Phys. Rev. Lett*., 1995, **75**, 858.
10. Omeltchenko, A., Nakano, A. and Kalia, R. K., *Structure, Mechanical Properties, and Thermal Transport in Microporous Silicon Nitride via Parallel Molecular Dynamics*, (MRS proc., 1996), Vol. 408, p. 175.
11. Vashishta, P., Nakano, A., Kalia, R. K. and Ebbsjö, I., Crack propagation and fracture in ceramic films—million atom molecular dynamics simulations on parallel computers. *Mat. Sci. Eng*., 1996, **B37**, 56.
12. Nakano, A., Kalia, R. K. and Vashishta, P., Dynamics and morphology of brittle cracks: a molecular-dynamics study of silicon nitride. *Phys. Rev. Lett*., 1995, **75**, 3138–3141.
13. Tsuruta, K., Omeltchenko, A., Kalia, R. K. and Vashishta, P., Early stages of sintering of silicon nitride nanoclusters: a molecular-dynamics study on parallel machines. *Europhys. Lett*., 1996, **33**, 441–446.
14. Kalia, R. K., Nakano, A., Tsuruta, K. and Vashishta, P., Morphology of pores and interfaces and mechanical behavior in nanocluster-assembled silicon nitride ceramic. *Phys. Rev. Lett*., 1997, **78**, 689.
15. Stillinger, F. H. and Weber, T. A., Computer simulation of local order in condensed phases of silicon. *Phys. Rev. B*, 1985, **31**, 5262.
16. Zhao, G. L. and Bachlechner, M. E., Electronic structure and charge transfer in α- and β-Si_3N_4 and at the Si(111)/Si_3N_4(001) interface. *Phys. Rev. B*, 1998, **58**, 1887–1895.
17. Kato, K., Inoue, Z. and Kijima, K., *J. Am. Ceram. Soc*., 1975, **58**, 90.
18. Senemaud, C., Driss-khodja, M. and Gheorghiu, A., *J. Appl. Phys*., 1993, **74**, 5042.
19. Stesmans, A. and Gorp, G. V., $Si{\equiv}Si_3$ defect at thermally grown (111)Si/Si_3N_4 interfaces. *Phys. Rev. B*, 1995, **52**, 8904–8920.
20. Bachlechner, M. E., Omeltchenko, A., Nakano, A., Kalia, R. K., Vashishta, P., Ebbsjö, I., Madhukar, A. and Messina, P., Multimillion-atom molecular dynamics simulation of atomic stresses in Si(111)/Si_3N_4(0001) nanopixels. *Appl. Phys. Lett*., 1998, **72**, 1969–1971.
21. Tuckerman, M. and Berne, B. J., Reversible multiple time scale molecular dynamics. *J. Chem. Phys*., 1992, **97**, 1990–2001.